Effects of Hydrogen Bonding and Structure of the Accessory Bacteriochlorophylls on Charge Separation in *Rb. capsulatus* Reaction Centers†

Lei Chen,‡ Dewey Holten,§ David F. Bocian,*,‡ and Christine Kirmaier*,§

Department of Chemistry, University of California, Riverside, California 92521-0403, and Department of Chemistry, Washington University, St. Louis, Missouri 63130-4899

Received: January 6, 2004; In Final Form: March 25, 2004

Histidine residues have been introduced into *Rb. capsulatus* reaction centers at M-polypeptide position 201 and at L-polypeptide position 174 to engender hydrogen bonds to the ring-V keto groups of the accessory bacteriochlorophyll cofactors B_A and B_B, respectively. Resonance Raman studies indicate that both mutations result in hydrogen-bonding interactions, as well as significant perturbations to the structure of the bacteriochlorophyll macrocycles. Nonetheless, ultrafast transient absorption measurements show that the structural/energetic effects of the mutations cause only minor changes in the primary photochemistry.

Introduction

The reaction center (RC) is a membrane-bound protein responsible for the initial charge-separation process in photosynthesis.[1] Purple bacterial RCs contain four bacteriochlorophylls (BChl's), two bacteriopheophytins (BPh's), two quinones (Q_S), and a non-heme iron arranged in two polypeptides designated L and M. Two of the BChl's form a dimer (P), which is the special pair primary electron donor. The X-ray crystal structures of RCs from two purple bacteria (*Rhodobacter sphaeroides* and *Blastochloris viridis*) reveal that P, the cofactors, and the L and M polypeptides are arranged with approximate C_2 symmetry.[2] In wild-type RCs, only one branch (designated A) of the symmetry-related A/B pair is functional (see Figure 1). This branch contains an accessory bacteriochlorophyll B_A, bacteriopheophytin H_A, and quinone Q_A. The B_A cofactor plays a dual role (as a superexchange mediator and as a discrete chemical intermediate) in the initial electron transfer from the singlet excited state of P (P*) to H_A. In wild-type RCs, it appears that $P^+B_A^-$ is slightly below P* in free energy, whereas $P^+B_B^-$ is above P*, as indicated in Figure 1. This difference contributes significantly to the unidirectionality of electron transfer to the A branch in wild-type RCs.[3−15]

A variety of amino acid mutations have been made in the RC protein that affect the free energies of the charge-separated states and the rates and yields of charge separation. Such changes are well documented to derive from cofactor−protein interactions such as formation/loss of hydrogen bonds to the pigments and/or from the effects of polar or ionizable residues such as Tyr/Phe or Asp/Glu, and they can give rise to electron transfer down the normally inactive B side of the RC.[11−15] The Glu/Asp residues are particularly interesting in that they have been found to either raise or lower the free energies of charge-separated states. For example, the native Glu residue at position L104 near H_A and an Asp residue at position M131 (introduced by mutagenesis) near H_B have been shown to form hydrogen bonds to these pigments, lowering the free energies of the corresponding $P^+H_A^-$ and $P^+H_B^-$ states.[3a,16−18] In contrast, Asp residues at M201 or L121, which are near B_A and H_A, respectively, appear to raise the free energies of the corresponding $P^+B_A^-$ or $P^+H_A^-$ states based on the effects on the electron-transfer reactions.[10c,12,19,20] These effects are most readily explained if the Asp residues are deprotonated and negatively charged.

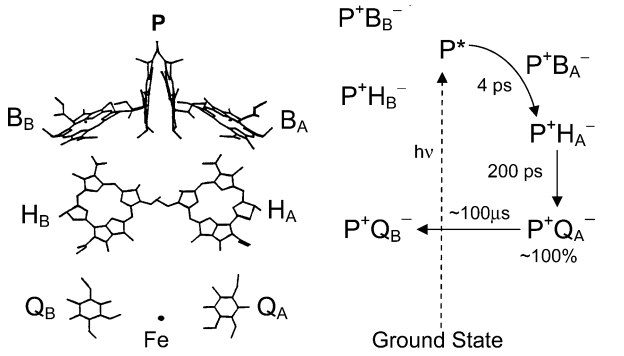

Figure 1. Cofactor arrangement and energy-level diagram for the RC.

His replacements have been used extensively around P to form hydrogen bonds to the dimer and increase its oxidation potential.[21,22] The change in the P/P^+ oxidation potential is 50−80 meV when the H-bond is to the C_9═O group in ring V of one BChl of P. His residues have also been exploited to great success in removing or providing a coordinating Mg ligand on the BChl's, with the resulting pigment change of BChl to BPh or vice versa.[10,13,23,24d] There has been much less exploration of His residues as a means of providing hydrogen bonds to the accessory BChl's or BPh's. Herein, we assess the effects of changing residues M201 and L174 to His in *Rb. capsulatus* RCs. These two residues are symmetry-related and close enough to B_A and B_B, respectively, to form a hydrogen bond to the pigment at the C_9═O group in ring V. In addition, or alternatively, the relatively large side chain of the His residue has the potential to cause significant structural changes on the BChl's due to steric interactions.

To assay the effects of the His replacements at positions M201 and L174, we have examined the RCs using both picosecond time-resolved transient absorption (TA) spectroscopy and static resonance Raman (RR) spectroscopy. The TA measurements

† Part of the special issue "Gerald Small Festschrift".
* To whom correspondence should be addressed.
‡ University of California.
§ Washington University.

10.1021/jp049939n CCC: $27.50
Published on Web 05/18/2004

probe the kinetics of the charge-separation process, whereas the RR measurements examine hydrogen bonding and structural perturbations to the BChl macrocycle. The TA measurements were performed on the double mutant G(M201)H/L(M212)H (denoted HH) and on the quadruple mutant M(L174)H/F(L181)Y/Y(M208)F/L(M212)H (denoted HYFH). The RR measurements were made on the HH and single M(L174)H mutants. The rationale for using the double and quadruple mutants is as follows:

(1) Genetically modified RCs with the template L(M212)H background were used to examine charge-separation kinetics because this mutation results in the incorporation of a BChl pigment (denoted β) in place of H_A.[10] This change results in a clean spectroscopic signature of the Q_x band of H_B by which electron transfer to this B-side pigment can be probed in TA experiments.[12]

(2) A study of the HH mutant is particularly interesting in the context of previous work on the G(M201)D/L(M212)H mutant (denoted DH). In the DH mutant, the rate of initial charge separation to the A branch is significantly lower than that in the L(M212)H mutant RC owing to a higher free energy of $P^+B_A^-$. This, in turn, results in ~15% yield of B-side electron transfer.[12a] In contrast, a hydrogen bond to B_A should lower the free energy of $P^+B_A^-$. This energetic change plausibly could either increase or decrease the rate of initial charge separation to the A side (compared to the H mutant). The direction of the change would depend significantly on the extent of the mixing between $P^+B_A^-$ and $P^+\beta^-$, the attendant effects on the relative contributions of $P^+B_A^-$ as a discrete intermediate and/or superexchange mediator, and the relationships between the free energy gaps and reorganization energies for the processes. States $P^+B_A^-$ and $P^+\beta^-$ are very close in free energy in the L(M212)H mutant (estimated to be within 50−100 meV of each other[10c,12c]). Thus, a possible extreme outcome of adding a hydrogen bond to B_A in the HH mutant is that $P^+B_A^-$ could become the lower-energy state and be a trap (in the sense of inhibiting further electron transfer to the β pigment and subsequently to Q_A), much the same as Katilius et al. have found on the B side upon the change of B_B to a BPh pigment.[13a,b]

(3) In the case of the HYFH mutant, the F(L181)Y/Y(M208)F/L(M212)H background (denoted YFH) was utilized because this triple mutant exhibits a large (30%) yield of $P^+H_B^-$ due to simultaneous lowering of the free energy of $P^+B_B^-$ and raising of the free energy of $P^+B_A^-$.[12d] If the added His at position L174 forms a hydrogen bond to B_B, the free energy of $P^+B_B^-$ would be further lowered and expected to result in an increased yield of $P^+B_B^-$, owing to an increased rate of charge separation to the B side. Again, there is the extreme possibility that, in the HYFH mutant, a hydrogen bond to B_B could result in $P^+B_B^-$ being lower in free energy than $P^+H_B^-$. This scenario is possible because the F(L181)Y mutation already significantly lowers the free energy of $P^+B_B^-$ compared to its position in wild-type RCs.[4a,b,5,8]

The combination of the TA and RR studies affords the possibility of probing all of the scenarios regarding hydrogen bonding and or/structural changes to the accessory BChl's and their effects on the free energy ordering of the charge-separated states and branching of initial charge separation to the A and B sides of the RC.

Materials and Methods

The HH mutant was constructed similarly to the DH mutant reported previously,[12a] except that the codon replacement at M201 was CAC, coding for a His residue. The L-gene mutation at 174 utilized a codon replacement of ATG to CAC. This change was made in the native wild-type L gene and also in an L gene bearing the F(L181)Y mutation previously made. From these intermediate forms, the single M(L174)H mutant and HYFH mutants were constructed. Codon changes in the DNA were made using Stratagene's Quick Change mutagenesis kit according to kit directions. The final mutants are derived from conjugation with the U43 strain of *Rb. capsulatus* originally developed by Youvan and co-workers.[24] We also have used their original pU2924 plasmid, but as further modified by Laible and Hanson[14a] to have a seven-residue histidine tag added to the carboxyl terminus of the M polypeptide. RC isolation and purification followed standard protocols for His-tagged RC protein and utilized the detergent LDAO to solubilize the RCs from the photosynthetic membranes.[14]

The TA measurements were carried out on an apparatus that utilizes ~130-fs excitation and white-light probe flashes. The samples (2.5−3-mL volumes of 25−35 μM RCs in 0.05% LDAO/100 mM Tris pH 7.8/100 mM NaCl) were held in an ice-cooled reservoir and flowed through a 2-mm-path-length cell. This arrangement maintained a sample temperature of ~10 °C. Further details of the TA instrumentation and data analysis procedures can be found elsewhere.[10c,25]

The RR measurements were carried out on optically dense (OD ≈ 1.0/mm at 800 nm) frozen snowy-glass samples at 25 and 250 K with Q_A prereduced by the addition of L-ascorbic acid before freezing. Temperature control was achieved by mounting the sample on a cold tip of a closed-cycle refrigeration system (ADP Cryogenics, DE-202 Displex). The RR spectra were obtained using a red-optimized triple spectrograph and detection system that has been previously described.[16] A Ti:sapphire laser (Coherent 890) pumped by an Ar ion laser (Coherent Innova 400-15UV) served as the excitation source. The laser power was typically ~1.0−1.5 mW. The power density on the sample was adjusted by defocusing the incident beam. Each RR data set was obtained with 4 h of signal average. The data acquisition time for an individual scan was dictated by the level of background fluorescence from a particular sample. These times ranged from 10 to 20 s. Because the Q_y-excitation RR spectra were superimposed on an emission background, all of the RR spectra were acquired using the shifted-excitation Raman difference spectroscopic (SERDS) technique.[26] The application of the SERDS method has been discussed in a number of earlier publications.[15,16,20,26b,27] Briefly, data sets are acquired at two excitation wavelengths that differ by a small wavenumber increment (typically 10 cm^{-1}) and subtracted to yield a background-free RR difference (SERDS) spectrum. The normal RR spectrum is then reconstructed from the SERDS data by fitting the latter to a series of derivative-shaped functions of arbitrary frequency, amplitude, and width. The frequencies marked in Figures 5−8 below correspond to the positions of the bands used in the fits and, thus, do not necessarily correspond to the peak maxima for overlapping bands. In addition, certain bands are marked that are not clearly resolved in the spectra. These bands are indicated because their inclusion noticeably improved the quality of the fits to the SERDS data.

Results and Discussion

TA Meaurements. Excitation of HH RCs with a 130-fs 590-nm flash produces (following ultrafast energy transfer) the excited singlet state of the primary donor, P* (0.5-ps spectrum in Figure 2). The transient absorption difference spectrum of P* displays bleaching of the 850-nm ground-state absorption

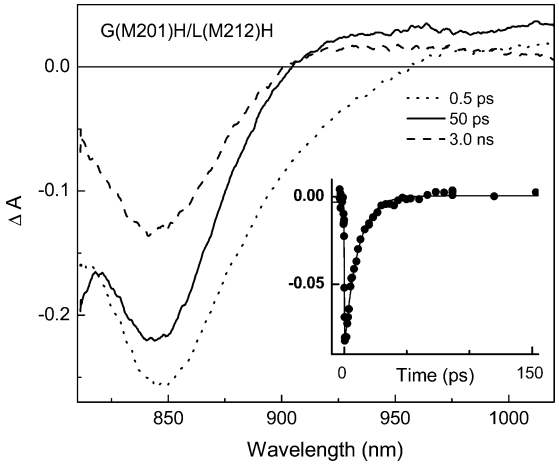

Figure 2. Transient absorption difference spectra in the P-bleaching and P* stimulated emission region for the G(M201)H/L(M212)H (HH) mutant at selected times following excitation with a 130-fs excitation flash at 590 nm. The kinetic trace and single-exponential fit ($\tau \approx 11$ ps) at 900−910 nm are shown in the inset.

band of P and concomitant stimulated emission from P* on the long-wavelength side of the P bleach. The kinetic profile of the decay of the stimulated emission averaged between 900 and 910 nm is shown in the inset of Figure 2. A fit of these data to the instrument response plus a single exponential plus a constant gives a time constant of 10.9 ± 0.6 ps for P* decay (solid curve in Figure 2, inset). A slightly better fit with time constants of ∼9 and ∼24 ps with relative contributions of 75 and 25%, respectively, is obtained from a two-exponential fit. The data in the 900−910-nm interval can be most cleanly associated solely with P* decay, largely free of spectral contributions from P-bleaching recovery or electron-transfer processes such as $P^+\beta^- \rightarrow P^+Q_A^-$. Thus, in the simplest model, 900−910-nm kinetic data should reflect the P* lifetime and be a single exponential.

The spectra in Figure 2 clearly show that there is extensive decay of P bleaching (signifying ground-state recovery) during the ∼3-ns time course of the experiments. The data throughout the P-bleaching region were averaged in 10-nm intervals between 840 and 900 nm and fit to the instrument response plus two exponentials plus a constant, yielding (average) time constants of 11 ± 2 and 380 ± 60 ps. On the blue side of the P bleaching (e.g., 840−850 nm), little contribution from P* stimulated emission is expected. The fact that there is an 11-ps component here indicates that some ground-state recovery occurs during the P* lifetime. From the preexponential factors of the two-exponential fit, we estimate the yield of direct decay of P* to the ground state to be ∼5%. This value is slightly larger than is seen for the L(M212)H single mutant (≤5%) and slightly less than that seen for the DH mutant (∼15%). We similarly estimate the overall yield of $P^+Q_A^-$ to be ∼50% for the HH RC. This latter value ignores any potential contribution to P bleaching due to electron transfer to the B side (and formation of $P^+H_B^-$, which would decay only partially on the time scale of the measurements). However, as shown next, the B-side yield in this mutant is estimated to be only ∼10%. The yield of $P^+Q_A^-$ in the L(M212)H mutant was found previously to be ∼70%.[12b] Figure 3B shows the maximal bleaching of the 527-nm Q_x band of H_B in HH RCs and compares it to the maximal bleaching of the H_B Q_x band found previously for L(M212)H and DH RCs. These comparisons are made with reference to identical magnitudes of P bleaching in the initial P* spectra, i.e., to the same initial P* concentration (Figure 3A). We have previously estimated the magnitude of the 527-nm bleaching in the L(M212)H and DH mutants to correspond to ∼5 and ∼15%

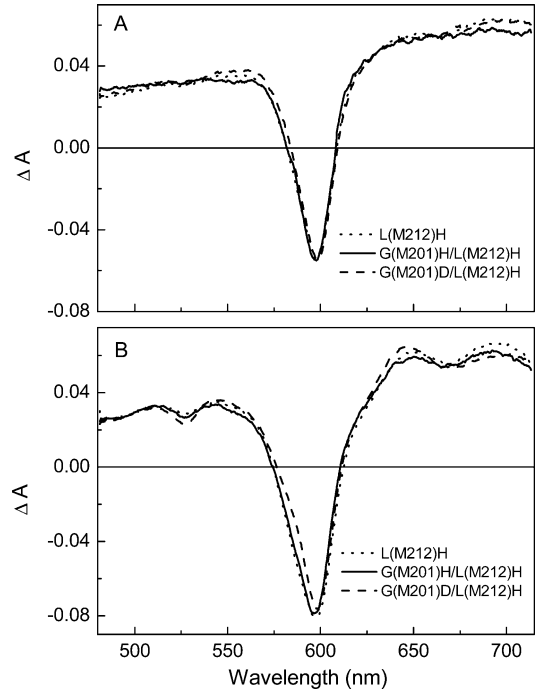

Figure 3. Comparison of the transient absorption difference in the Q_x-bleaching region for the indicated RCs following excitation with a 130-fs flash at 850 nm. Panel A shows spectra for P* immediately after excitation after normalizing (with <10% corrections due to experimental conditions) to the same initial P bleaching at ∼600 nm. Panel B shows spectra acquired at a delay time corresponding to about three P* lifetimes (20−50 ps) where the maximum concentration of $P^+H_B^-$ and the associated bleaching at 527 nm should be observed.

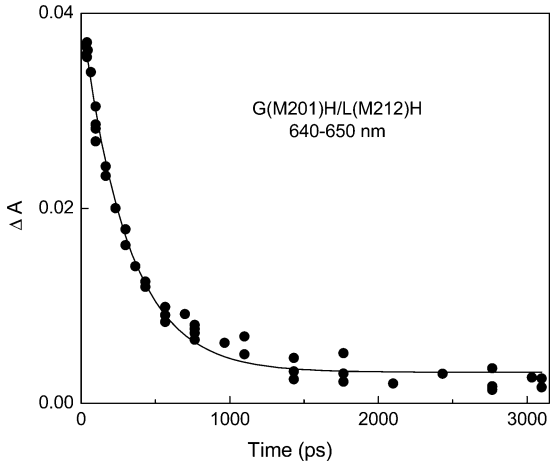

Figure 4. Kinetic profile and single-exponential fit ($\tau \approx 310$ ps) for the anion-region decay at 640−650 nm obtained using excitation of G(M201)H/L(M212)H (HH) RCs with a 130-fs flash at 850 nm.

yields of $P^+H_B^-$, respectively.[12a−c] It can be seen in Figure 3B for the HH mutant that the 527-nm bleaching is essentially the same magnitude as that found in the L(M212)H mutant, possibly a few percent larger, but smaller than that found for the DH mutant. Thus we estimate the yield of B-side electron transfer in the HH mutant to be ∼10%.

The spectra in Figure 3B show features between 640 and 700 nm that are consistent with the formation of a mixture of the A-side anions of B_A/β and the B-side H_B anion (see, e.g., spectra in ref 12d). The H_B anion is known to have a peak near 640−650 nm and would, therefore, be most pronounced at these wavelengths. Figure 4 shows the decay portion of the kinetic data between 640 and 650 nm, along with a single-exponential fit. The resulting time constant is 307 ± 15 ps, with an average

value of 300 ± 20 ps obtained from similar fits of the data in 10-nm intervals over the entire region between 640 and 700 nm. Given that there is an admixture of states present at the start of this decay (i.e., formed from P*) consisting of $P^+\beta^-$/$P^+B_A^-$ on the A side and $P^+H_B^-$ on the B side, the single-exponential fits are quite good. This is expected, however, because the $P^+H_B^-$ yield is only 5−10%. We have shown elsewhere that the lifetime of this state (in the absence of electron transfer to Q_B) is on the order of 1−5 ns.[12b−d,14b] A 5−10% contribution of this kinetic component would thus easily account for the small deviation from a pure exponential seen in Figure 4. Fitting the data with a fixed component of 1−5 ns improves the fit, but determining an accurate value for this component is difficult even when the yield of $P^+H_B^-$ is much larger than it is for the HH mutant (see, e.g., ref 14b) and is beyond the scope of this work.

The key point of the results described above is that the time constant of the major component determined from the anion-region kinetic data agrees well with the longer component of the P-bleaching decay kinetics, giving a ∼300-ps lifetime for the A-side admixture of $P^+\beta^-$/$P^+B_A^-$. This value is slightly longer than the ∼230-ps lifetime determined previously for the single L(M212)H mutant.[10c] As noted above, the yield of $P^+Q_A^-$ is somewhat smaller in the HH mutant than in the L(M212)H mutant. The lifetime and relative branching pathways of the decay of $P^+\beta^-$/$P^+B_A^-$ are well established to be highly sensitive to the relative free energies (and thus mixing) of these states.[10,12c] Thus, the TA data on the HH mutant suggests that the His at M201 has affected the B_A pigment and modestly altered the electron-transfer and charge-recombination kinetics in this RC.

For the HYFH mutant, TA experiments were performed only in the Q_x region. We find that the amplitude of the bleaching of the Q_x band of H_B is identical within experimental error to that found previously for the YFH mutant (data not shown).[12d] Thus, as for the HH mutant, a conclusion of the TA results is that, if M(L174)H is hydrogen bonded to B_B, the effect on the free energy of $P^+B_B^-$ is not large enough to significantly enhance initial charge separation to the B side. On the other hand, the magnitude of the 600-nm P bleaching at ∼3 ns is about 40% smaller in the HYFH mutant than in the YFH mutant, which *is* evidence for a change in the free energy of $P^+B_B^-$ that alters the decay properties of $P^+B_B^-$/$P^+H_B^-$. Finding definitively that there is a change (lowering) in the free energy of $P^+B_B^-$ but with no resultant change (increase) in the yield of $P^+H_B^-$ would be interesting and would address the degree to which electronic couplings complement free energy relationships in governing the directionality of electron transfer from P*.

RR Spectra. The high-frequency regions (1500−1745 cm^{-1}) of the Q_y-excitation (λ_{ex} = 800 nm) RR spectra for the HH and M(L174)H RCs are shown in Figure 5; the low-frequency regions (90−400 cm^{-1}) of the spectra for the two mutants are shown in Figure 6. The high-frequency spectra shown were obtained at 250 K, whereas the low-frequency spectra shown were obtained at 25 K. The spectra at these temperatures are presented because a study wherein data were obtained at a number of temperatures in the 25−250 K range revealed that the spectral quality was best at these temperatures (250 K, high-frequency region; 25 K, low-frequency region), mainly because of the relative contributions of fluorescence backgrounds. In each of the spectra, the top trace is the raw (unsmoothed) SERDS data. The second trace is the fit of the SERDS data. The trace at the bottom is the SERDS residual (SERDS minus fit). The relatively small residuals compared with the SERDS intensities are indicative of the excellent fidelity of the fits. The high- and low-frequency regions of the reconstructed RR spectra of the HH and M(L174)H RCs are shown in Figures 7 and 8.

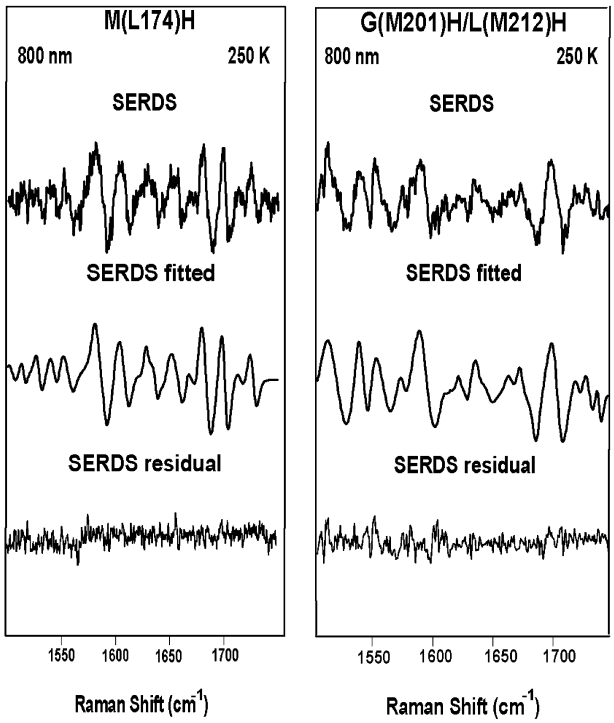

Figure 5. High-frequency regions (1500−1745 cm^{-1}) of the Q_y-excitation (λ_{ex} = 800 nm) RR spectra of the M(L174)H (left panel) and G(M201)H/L(M212)H (HH) (right panel) RCs obtained at 250 K. In each panel, the top trace is the SERDS data, the middle trace is the fit of the SERDS data, and the bottom trace is the SERDS residual (observed − fit).

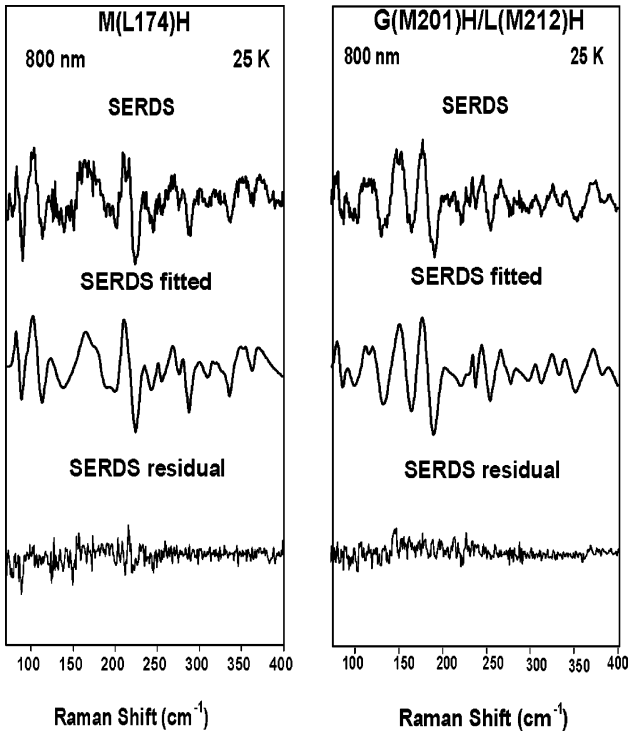

Figure 6. Low-frequency regions (90−400 cm^{-1}) of the Q_y-excitation (λ_{ex} = 800 nm) RR spectra of the M(L174)H (left panel) and G(M201)H/L(M212)H (HH) (right panel) RCs obtained at 25 K. In each panel, the top trace is the SERDS data, the middle trace is the fit of the SERDS data, and the bottom trace is the SERDS residual (observed − fit).

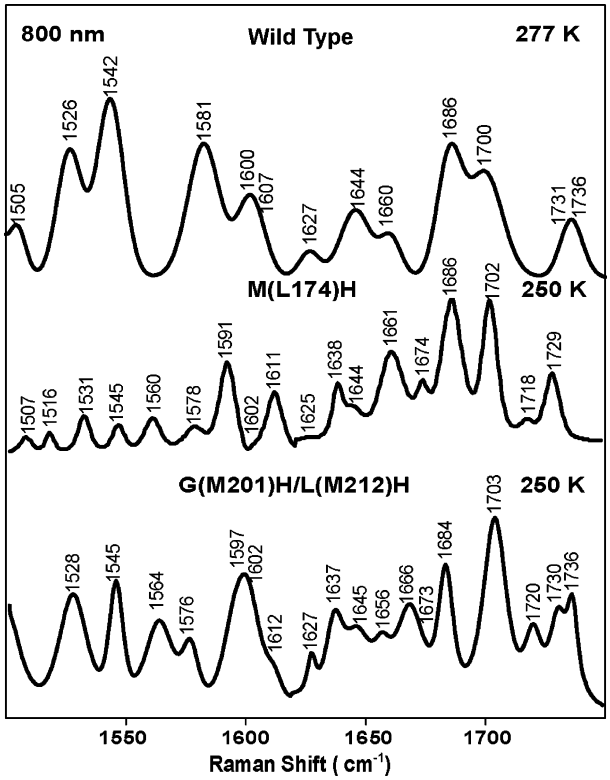

Figure 7. Comparison of the high-frequency regions of the Q_y-excitation RR spectra of the BChl's of wild-type, M(L174)H, and G(M201)H/L(M212)H (HH) RCs. The spectra of the two mutants were reconstructed from the fitted data in Figure 5. The spectra of the wild type RC were taken from ref 20a.

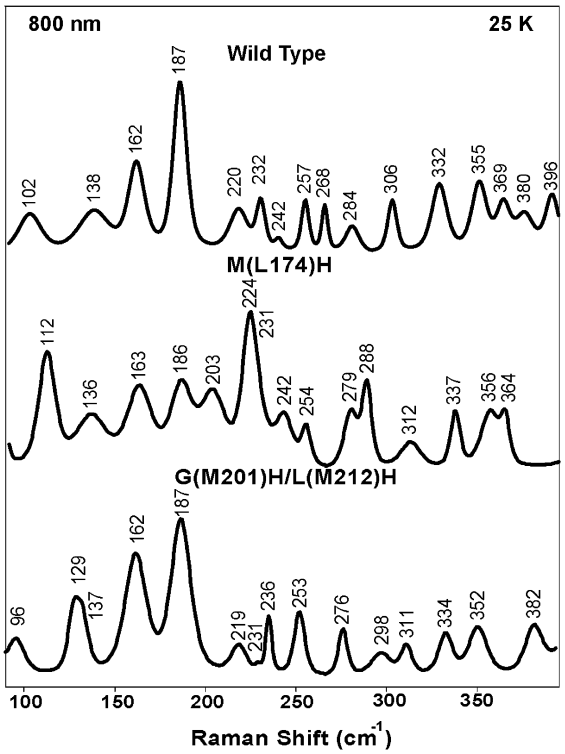

Figure 8. Comparison of the low-frequency regions of the Q_y-excitation RR spectra of the BChl's of wild-type, M(L174)H, and G(M201)H/L(M212)H (HH) RCs. The spectra of the two mutants were reconstructed from the fitted data in Figure 6. The spectra of the wild type RC were taken from ref 18a.

For comparison, the RR spectra of wild-type *Rb. capsulatus* RCs are also included in these figures.

The objectives of the RR studies were to assess whether His replacements at positions M201 and L174 result in hydrogen bonds to the C_9═O groups in ring V of the accessory BChl's B_A and B_B, respectively, and to determine whether the presence of the bulky imidazole side chain results in structural perturbations of the macrocycle. With this in mind, we focus on the frequencies of the key spectral features in comparison to the analogous modes of wild-type RCs. The frequencies of the vibrations reflect the properties of the ground electronic states of the cofactors. On the other hand, the relative RR intensities are determined by the excited-state properties and the wavelength of the excitation with respect to the Q_y absorption contour. Previous studies have shown that the RR intensities for a cofactor can be significantly affected by the alteration of neighboring protein residues even when the ground-state vibrational frequencies of the cofactor are not affected to any appreciable extent.[19,20]

The vibrations enhanced with Q_y excitation include carbonyl, ring skeletal, and substituent modes.[16,28,29] RR bands that can be assigned to the νC═O vibrations of the C_{2a}-acetyl and C_9═O carbonyl groups are observed in the highest-frequency spectral region, above 1650 cm^{-1}.[16,29] RR bands that can be assigned to stretching vibrations of the C_aC_m and unsaturated C_bC_b bonds of the macrocycle dominate the 1550−1650 cm^{-1} region.[16] RR bands due to deformations of the macrocycle and the peripheral substituent groups are the principal contributors to the low-frequency spectrum, below 500 cm^{-1}.[28] The RR bands of the accessory BChl's of the HH and M(L174)H mutants can be assigned via analogy to those of the wild-type RCs. The assignments for selected high- and low-frequency modes of the pigments in the mutant and wild-type RCs are summarized in Table 1. The assignments can be correlated with the structure of the BChl macrocycle via comparison with Figure 9. The salient features of the RR spectra of the HH and M(L174)H mutants are summarized as follows:

In the case of wild-type RCs, the C_9═O groups of both B_A and B_B are not hydrogen bonded, and the νC_9═O vibrations are not resolved (from each other) and occur near 1686 cm^{-1} (Figure 7). Both the HH and M(L174)H mutants exhibit an RR band near 1686 cm^{-1} that is due to the νC_9═O mode of a non-hydrogen-bonded keto group. However, the M(L174)H mutant exhibits a second RR band at ∼1674 cm^{-1} that is absent in the spectrum of the wild type. Such a feature is not cleanly resolved for the HH mutant; however, the fits to the SERDS data indicate that a band is also present near this frequency, but is overlapped with a lower-frequency feature. The ∼1674 cm^{-1} RR bands of the HH and L(M174)H RCs can be assigned to the νC_9═O vibrations of hydrogen-bonded keto groups on the B_A and B_B cofactors, respectively. The downshift of ∼10 cm^{-1} is consistent with that observed in other genetically modified RCs wherein hydrogen bonds are formed to C_9═O groups of the bacteriochlorin pigments.[17,30,31]

Inspection of the high-frequency RR spectra for the M(L174)H and HH mutants reveals additional differences compared with the wild type RC (Figure 7). For example, both the HH and M(L174)H RCs exhibit a RR band at ∼1638 cm^{-1} in addition to a feature at ∼1644 cm^{-1}. The former band is absent in the wild-type spectrum, whereas the latter is due to the [$\nu C_aC_m(\gamma)$, νC_9═O] modes of B_A and B_B, which are overlapped and not resolved. Plausibly, the ∼1638 cm^{-1} band observed for the two mutants is a perturbed [$\nu C_aC_m(\gamma)$, νC_9═O] vibration in either the B_A or B_B pigment, causing splitting from the feature at ∼1644 cm^{-1}. This vibration is of mixed parentage and contains both stretching character of the methine bridge that is included

TABLE 1: Frequencies (cm^{-1}) and Assignments for Selected RR Bands of the B_A and B_B[a]

description[b]	M(L174)H		G(M201)H/L(M212)H (HH)		Wild-Type
	B_A	B_B	B_A	B_B	$B_{A,B}$
$\nu C_9{=}O$	1686	1674	1673	1684	1686
$\nu C_{2a}{=}O$	1661		1656/1666		1660
[$\nu C_aC_m(\gamma)$, $\nu C_9{=}O$]	1644	1638	1637	1645	1644
[νC_bC_b(III), $\nu C_aC_m(\gamma)$]	1625		1627		1627
$\nu C_aC_m(\alpha,\beta,\gamma,\delta)$	1611		1612		1607
[$\nu C_aC_m(\delta)$, νC_bC_b(I)]	1602		1697	1602	1600
νMgN_{his}	242		236	241	242
δC_bC_{alkyl}(I,II,IV)	231		231		232
[δC_bCH_3(I), δC_bC_{alkyl}(II,IV)]	224		219		220
[δC_bC_{alkyl}(II,IV), $\delta C_{10}C_{carbo}$,$\delta C_9{=}O$]	186	203	187		187
γMg_{dome}	136		129	137	138

[a] Taken from refs 16 and 28; a single frequency indicates that the bands for B_A and B_B are coincident. [b] Mode descriptions are as follows: ν = stretch, δ = in-plane deformation, γ = out-of-plane deformation. The designators C_a, C_b, C_m, I−IV, and α, β, γ, δ refer to Figure 9.

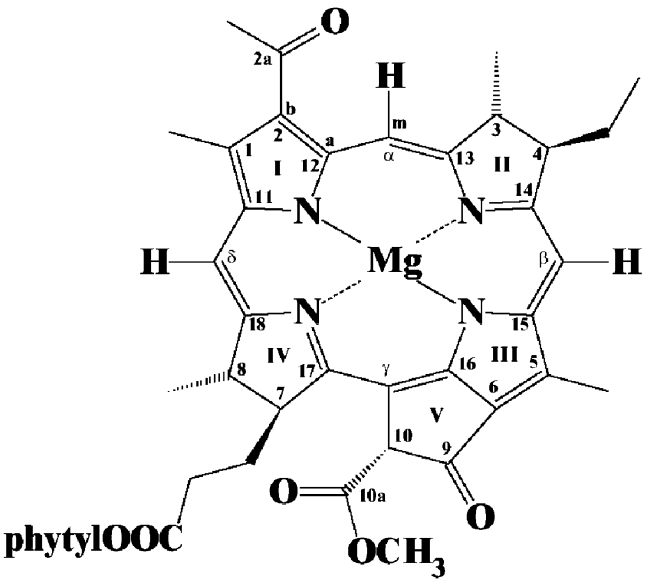

Figure 9. Structure and labeling scheme for BChl a.

in ring V and $C_9{=}O$ stretching (see Figure 9). The downshift of this mode suggests structural perturbations (above and beyond hydrogen bonding) in ring V resulting from the placement of His nearby. The RR spectra of both mutants in the 1590−1615 cm^{-1} region are also different from one another and different from those of wild-type. Several bands appear in this region that are due to ring-skeletal modes (Table 1). The spectral changes in the mutants suggest additional structural perturbations on the core of the BChl macrocycle.

Inspection of the low-frequency RR spectra for the M(L174)H and HH mutants also reveals differences between the two mutants and the wild type RC (Figure 8). For example, in the L(M174)H mutant, a band appears at ∼203 cm^{-1} that is not observed for either the wild type RC or the HH mutant. Concomitantly, the intensity of the 187 cm^{-1} band of the M(L174)H mutant is significantly lower than that of either the wild type RC or the HH mutant. Together, these features of the RR spectra suggest that the 203 cm^{-1} band of the M(L174)H mutant could be due to a perturbed [δC_bC_{alkyl}(II,IV), $\delta C_{10}C_{carbo}$,$\delta C_9{=}$O] mode of B_B that is upshifted from its coincident (in wild type) B_A partner. These low-frequency spectral features of the M(L174)H mutant reflect structural perturbations of the BChl ring skeleton. In the case of the HH mutant, spectral differences from wild type [and the M(L174)H mutant] are apparent in the 220−240 cm^{-1} region. This region includes the νMgN_{his} vibration, which occurs at ∼242 cm^{-1} in the wild type RC. In the HH mutant, a band is observed at 236 cm^{-1} that could be a perturbed νMgN_{his} mode of B_A. [The unperturbed B_A analogue is not clearly observed with 800-nm excitation; however, a band is observed at this frequency in spectra obtained with 805-nm excitation (not shown).] The shift in the νMgN_{his} vibration of B_A in the HH mutant signals a perturbation of the core of the BChl macrocycle.

Relation of Structure and Function in the HH and M(L174)H RCs. The charge-separation kinetics along with the vibrational characteristic of the BChl's in the HH and M(L174)H mutants can be used to construct a more complete relationship between the structural and functional characteristics of the RCs. The picture that emerges is that the His mutations at M201 and L174 result in hydrogen bonds to B_A and B_B, respectively. As noted above, previous work[21,22] on adding hydrogen bonds to the BChl's of P suggests that formation of a hydrogen bond to the $C_9{=}O$ group of ring V of either B_A or B_B should make these cofactors easier to reduce by 50−80 mV and result in a 50−80 meV stabilization of the corresponding P^+B^- state. Such stabilization could, in principle, increase the yield of electron transfer to the B side in the HH mutant via a decreased rate of A-side charge separation and in the HYFH mutant via an increased rate of B-side charge separation. The His mutations at M201 and L174 also result in structural perturbations to the BChl macrocycles both in the region of ring V and in the core. Regardless of these combined structural and energetic effects, the rates and yields of the initial stage of charge separation are altered only modestly for the HH mutant and virtually not at all for the HYFH mutant compared to reference RCs that lack the His replacements.

In considering the HH mutant, we begin with current estimates that $P^+B_A^-$ is 50−100 meV below P* in free energy (in wild type) and that $P^+\beta^-$ is 100−150 meV below P* (in the single L(M212)H mutant).[5b,12c] (For reference, $P^+H_A^-$ in wild-type RCs is thought to be 250−300 meV below P*.) Thus, the expected result for the HH mutant is that $P^+B_A^-$ will be lowered in free energy by 50−80 meV, placing it very close to $P^+\beta^-$. Although the precise energy relationship of the two states cannot be determined from this work, useful comparisons can be made to previous work on the F(L97)V/F(L121)D/L(M212)H mutant. In the latter RC, an Asp was added near ring V of the β pigment. The effects on the photochemistry indicate that this mutation raised the free energy of $P^+\beta^-$, placing it very close in free energy to $P^+B_A^-$.[12c] Thus, the F(L97)V/F(L121)D/L(M212)H mutant and the HH mutant studied here have in common that states $P^+\beta^-$ and $P^+B_A^-$ may be roughly isoenergetic, with the pair being 50−100 meV below P* in free energy in the F(L97)V/F(L121)D/L(M212)H mutant and 100−150 meV below P* in the HH mutant. The close energy proximity of $P^+\beta^-$

TABLE 2: Transient-State Lifetimes and Yields for *Rb. capsulatus* Wild-Type and Mutant RCs[a]

sample	τ P* (ps)	ground-state yield (%)	$P^+H_B^-$ yield (%)	P^+I^- yield (%)	τ P^+I^- (ps)	$P^+Q_A^-$ yield (%)
wild type	4.3 ± 0.3	0	0	100	175 ± 15	100
L(M212)H	8.5 ± 0.8	0	7	93	230 ± 30	70
G(M201)D/L(M212)H (DH)	15 ± 2	15	15	70	150 ± 30	70[b]
F(L97)V/F(L121)D/L(M212)H	10 ± 2	5	12	83	190 ± 30	40
G(M201)H/L(M212)H (HH)	11 ± 2	5	10	85	300 ± 40	50

[a] Errors in the yields are typically ±3%. The values for the first four entries are from refs 12a−c with a slightly revised value for the yield of state $P^+H_B^-$ in the L(M212)H RC. The A-side intermediate P^+I^- is $P^+H_A^-$ in the wild-type RC and an admixture of $P^+B_A^-$ and $P^+\beta^-$ in the other RCs. [b] A-side intermediate P^+I^- could decay up to 10% to the ground state, lowering the $P^+Q_A^-$ yield to 60%.

and $P^+B_A^-$ will result in even greater mixing (thermal or quantum) between the two states in these two mutants than in the L(M212)H RC.[10] In view of this discussion, it is not surprising that the P* lifetimes, the yield of B-side electron transfer, and the relative branching of the photochemistry from the mixed $P^+\beta^-/P^+B_A^-$ states are very similar in the HH and F(L97)V/F(L121)D/L(M212)H mutants, as is seen from the results collected in Table 2.

With regard to the specific issue of B-side electron transfer, the added hydrogen bond to B_A in the HH mutant increases the P* lifetime and the yield of $P^+H_B^-$ slightly. These effects can be understood if the lowered free energy of $P^+B_A^-$ (due to the hydrogen bond) slightly reduces the effective rate of electron transfer to the A side, making B-side electron transfer slightly more competitive. However, the apparent reduction in free energy of $P^+B_A^-$ is not large enough to move this state so far as to be a "trap" (i.e., significantly below $P^+\beta^-$). Taken as a whole, the results on the HH mutant reinforce the estimates for free energies of the A-side states and demonstrate consistency in the effects on the primary photochemistry of bringing states $P^+\beta^-$ and $P^+B_A^-$ closer in free energy by mutations near either electron carrier.

In the case of the HYFH mutant, the absence of any measurable effect on the yield of B-side electron transfer compared to the ~30% yield for the YFH benchmark RC[12d] is perhaps more surprising. The swap of M208 from Tyr to Phe is thought[4a,5a] to raise the free energy of $P^+B_A^-$ by ~100 meV, placing it very close to P* in free energy and possibly even slightly above P*. The free energy of $P^+B_B^-$ is estimated to be 100−200 meV above that of P*, so the swap of L181 from Phe to Try probably still leaves $P^+B_B^-$ above P* (see ref 12d for further discussion). The intent of the addition of a hydrogen bond to B_B was to drop this state below P* and thereby increase the rate and yield of B-side electron transfer to form $P^+H_B^-$. Clearly, the latter result is not obtained, as there is essentially no change compared to the YFH mutant. This negative result has several possible origins. One is that a hydrogen bond to B_B has only a small effect on the free energy of $P^+B_B^-$, rather than the anticipated value of 50−80 meV. Such a finding would indicate a difference between the A and B sides of the RC because hydrogen bonding to B_A does appear to affect the free energy of $P^+B_B^-$ by 50−80 meV. In this regard, Katilius et al. were unable to push the free energy of the $P^+\Phi_B^-$ state above that of $P^+H_B^-$ in their H(L182)L mutant (in which B_B is replaced with a Phe pigment denoted Φ_B) by adding neighboring Asp residues.[13e]

The results described above are in contrast to the generally more significant effects on the free energies and primary photochemistry elicited by the addition of hydrogen bonding or ionic residues near either B_A or H_A (or β) on the A-side of the RC.[10c,12a,c] These differences might result in part if the lower overall dielectric constant experienced by the cofactors on the B side of the RC[5a,7a] makes the electron-transfer rates less sensitive to hydrogen-bonding or electrostatic interactions compared to the A side. A tempered effect of B-side mutations such as those in the HYFH RC and in the RCs studied by Katilius et al.[13e] might also be providing experimental insights into the relative contributions of energetic and electronic coupling factors to the directionality of charge separation. An open question is the extent to which the relative electronic matrix elements compound the demonstrated importance of the relative free energies of the A- and B-side charge separated states in governing the directionality of electron transfer.

Finally, it is also noteworthy that the significant structural perturbations of the BChl macrocycles that result from the His replacements have little effect on the electron-transfer kinetics in the RCs. Regardless, these observations are similar to those that have been previously made on other types of RCs wherein the structure of the BChl or BPh macrocycle is significantly perturbed by mutations in the protein superstructure. These RCs include His mutants near H_A[23] and special pair cavity mutants,[32] with the nature of the axial ligands to the BChl's in P being altered in the latter. Together, the studies reported herein and this earlier work indicate that substantial structural perturbations that encompasses P, the accessory BChl's, and H_A have little effect on the functional characteristics of the RC. Collectively, these observations indicate that the RC is resilient to changes in the protein scaffolding that can alter the structure of the active cofactors.

Acknowledgment. This work was supported by Grant MCB-0314588 (D.H. and C.K.) and Grant GM-39781 (D.F.B.) from the National Institute of General Medical Sciences.

References and Notes

(1) (a) Deisenhofer, J., Norris, J. R., Eds. *The Photosynthetic Reaction Center*; Academic Press: San Diego, CA, 1993; Vol. II. (b) Blankenship, R. E., Madigan, M. T., Bauer, C. E., Eds. *Anoxygenic Photosynthetic Bacteria*; Kluwer Academic Publishers: Dordrecht, The Netherlands, 1995; pp 503−708. (c) Michel-Beyerle, M. E., Ed. *The Reaction Center of Photosynthetic Bacteria*; Springer: Berlin, 1996.

(2) (a) Deisenhofer, J.; Epp, O.; Miki, K.; Huber, R.; Michel, H. *Nature* **1985**, *318*, 618−624. (b) Yeates, T. O.; Komiya, H.; Chirino, A.; Rees, D. C.; Allen, J. P.; Feher, G. *Proc. Natl. Acad. Sci. U.S.A.***1988**, *85*, 7993−7997. (c) El-Kabbani, O.; Chang, C.-H.; Tiede, D.; Norris, J.; Schiffer, M. *Biochemistry* **1991**, *30*, 5361−5369. (d) Ermler, U.; Fritzsch, G.; Buchanan, S.; Michel, H. *Structure* **1994**, *2*, 925−936. (e) Deisenhofer, J.; Epp, O.; Sinning, I.; Michel, H. *J. Mol. Biol.* **1995**, *246*, 429−257.

(3) (a) Michele-Beyerle, M. E.; Plato, M.; Deisenhofer, J. Michel, H.; Bixon, M.; Jortner, J. *Biochim. Biophys. Acta* **1988**, *832*, 52−70. (b) Scherer P. O. J.; Fischer, S. F. *Chem. Phys.* **1989**, *131* 115−127. (c) Bixon, M.; Jortner, J.; Michel-Beyerle, M. E. *Biochim. Biophys. Acta* **1991**, *1056*, 301−315.

(4) (a) Warshel, A.; Creighton, S.; Parson, W. W. *J. Phys. Chem.* **1988**, *92*, 2694−2701. (b) Alden, R. G.; Parson, W. W.; Chu, Z.-T.; Warshel, A. *J. Am. Chem. Soc.* **1995**, *117*, 12284−12298. (c) Nagarajan, V.; Parson, W. W.; Gaul, D.; Schenck, C. C. *Biochemistry* **1993**, *32*, 12324−12336.

(5) (a) Gunner, M. R.; Nicholls, A.; Honig, B. *J. Phys. Chem.* **1996**, *100*, 4277−4291. (b) Gunner, M. R. *Curr. Top. Bioenergetics* **1991**, *16*, 319.

(6) (a) Thompson, M. A.; Zerner, M. C.; Fajer, J. *J. Am. Chem. Soc.* **1991**, *113*, 8210−8215. (b) Zhang, L. Y.; Friesner, R. A. *Proc. Natl. Acad. Sci. U.S.A.* **1998**, *95*, 13603−13605. (c) Kobalsov, D. Scherz, A. *J. Phys. Chem. B.* **2000**, *104*, 1802−1809. (d) Ivashin, N.; Kallebring, B.; Larsson, S.; Hansson, O. *J. Phys. Chem. B* **1998**, *102*, 5017−5022. (e) Pudak, M.; Pincak, R. *Chem Phys. Lett.* **2001**, *342*, 587−592.

(7) (a) Steffen, M. A.; Lao, K.; Boxer, S. G. *Science* **1994**, *264*, 810−816. (b) King, B. A.; McAnaney, T. B.; deWinder, A.; Boxer, S. G. *J. Phys. Chem.* **2001**, *105*, 1856−1862.

(8) Jia, Y.; DiMagno, T. L.; Chan, C.-K.; Wang, Z.; Du, M.; Hanson, D. K.; Schiffer, M.; Norris, J. R.; Fleming, G. R.; Popov, M. S. *J. Phys. Chem.* **1993**, *97*, 13180−13191.

(9) (a) Schmidt, S.; Artl, T.; Hamm, P.; Huber, H.; Nagele, T.; Wachtveitl, J.; Meyer, M.; Scheer, H.; Zinth, W. *Chem. Phys. Lett.* **1994**, *223*, 116−120. (b) Shkurapatov, A. Y.; Shuvalov, V. A. *FEBS Lett.* **1993**, *322*, 168−172. (b) Kennis, J. T. M.; Shkurapatov, A. Y.; van Stokkum, I. H. M.; Gast, P.; Hoff, A. J. Shuvalov, V. A.; Aartsma, T. J. *Biochemistry* **1997**, *36*, 16231−16238.

(10) (a) Kirmaier, C.; Gaul, D.; DeBey, R.; Holten, D.; Schenck, C. C. *Science* **1991**, *251*, 922−927. (b) Kirmaier, C.; Laporte, L.; Schenck, C. C.; Holten, D. *J. Phys. Chem.* **1995**, *99*, 8910−8917. (c) Heller, B. A.; Holten, D.; Kirmaier, C. *Biochemistry* **1996**, *35*, 15418−15427.

(11) (a) Kellogg, E. C.; Kolaczkowski, S.; Wasiewlewski, M. R. Tiede, D. M. *Photosynth. Res.* **1989**, *22*, 47−59. (b) Gray, K. A.; Weichtveitl, J. Oesterhelt, D. *Eur. J. Biochem.* **1992**, *207*, 723−731.

(12) (a) Heller, B. A.; Holten, D.; Kirmaier, C. *Science* **1995**, *269*, 940−945. (b) Kirmaier, C.; Weems, D.; Holten, D. *Biochemistry* **1999**, *38*, 11516−11530. (c) Roberts, J. A.; Holten, D.; Kirmaier, C. *J. Phys. Chem. B* **2001**, *105*, 5575−5584. (d) Kirmaier, C.; He, C.; Holten, D. *Biochemistry* **2001**, *40*, 12132−12139.

(13) (a) Katilius, E.; Turanchik, T.; Lin, S.; Taguchi, A. K. W.; Woodbury, N. W. *J. Phys. Chem. B* **1999**, *103*, 7386-7389. (b) Katilius, E.; Katiliene, Z.; Lin, S.; Taguchi, A. K. W.; Woodbury, N. W. *J. Phys. Chem. B* **2002**, *106*, 12344−12350. (c) Lin, S.; Katilius, E.; Haffa, A. L.; Taguchi, A. K.; Woodbury, N. W. *Biochemistry* **2001**, *40*, 13767−13773. (d) Haffa, A. L.; Lin, S.; Williams, J. C.; Taguchi, A. K. W.; Allen, J. P.; Woodbury, N. W. *J. Phys. Chem. B* **2003**, *107*, 12503−12510. (e) Katilius, E.; Babendure, J. L.; Katiliene, Z.; Lin, S.; Taguchi, A. K. W.; Woodbury, N. W. *J. Phys. Chem. B* **2003**, *107*, 12029−12034.

(14) (a) Laible, P. D.; Kirmaier, C.; Udawatte, C. S. M.; Hofman, S. J.; Holten, D.; Hanson, D. K. *Biochemistry* **2003**, *42*, 1718−1730. (b) Kirmaier, C.; Laible, P. D.; Hanson, D. K.; Holten, D. *Biochemistry* **2003**, *42*, 2016−3024.

(15) (a) deBoer, A. L.; Neerken, S.; deWijn, R.; Permentier, H. P.; Gast, P.; Vijgenboom, E.; Hoff, A. J. *Biochemistry* **2002**, *41*, 3081−3088. (b) deBoer, A. L.; Neerken, S.; deWijn, R.; Permentier, H. P.; Gast, P.; Vijgenboom, E.; Hoff, A. J. *Photosynth. Res.* **2002**, *71*, 221−239.

(16) Palaniappan, V.; Martin, P. C.; Chynwat, V.; Frank, H. A.; Bocian, D. F. *J. Am. Chem. Soc.* **1993**, *115*, 12035−12049 and references therein.

(17) Kirmaier, C.; Cua, A.; He, C.; Holten, D.; Bocian, D. F. *J. Phys. Chem. B* **2002**, *106*, 495−503.

(18) Muh, F.; Williams, J. C.; Allen, J. P.; Lubitz, W. *Biochemistry* **1998**, *37*, 13066−13074.

(19) Cua, A.; Kirmaier, C.; Holten, D.; Bocian, D. F. *Biochemistry* **1998**, *37*, 6394−6401.

(20) (a) Czarnecki, K.; Kirmaier C.; Holten, D.; Bocian, D. F. *J. Phys. Chem. A* **1999**, *103*, 2235−2246. (b) Kirmaier, C.; Laible, P. D.; Czarnecki, K.; Hata, A. N.; Hanson, D. K.; Bocian, D. F.; Holten, D. *J. Phys. Chem. B* **2002**, *106*, 1799−1808.

(21) (a) Murchison, H. A.; Alden, R. G.; Allen, J. P.; Peloquin, J. M.; Taguchi, A. K. W.; Woodbury, N. W.; Williams, J. C. *Biochemistry* **1993**, *32*, 3498−3505. (b) Peloquin, J. M.; Williams, J. C.; Lin, X.; Alden, R. G.; Taguchi, A. K. W.; Allen, J. P.; Woodbury, N. W. *Biochemistry* **1994**, *33*, 8089−8100. (c) Lin X.; Murchison, H. A.; Nagarajan V.; Parson W. W.; Allen J. P.; Williams, J. C. *Proc. Natl. Acad. Sci. U.S.A.* **1994**, *91*, 10265−10269. (d) Mattioli, T. A.; Lin, X.; Allen, J. P.; Williams, J. C. *Biochemistry* **1995**, *34*, 6142−6152. (e) Ivancich, A.; Mattioli, T. A.; Artz, K.; Wang, S.; Allen, J. P.; Williams, J. C. *Biochemistry* **1997**, *36*, 3027−3036.

(22) Spiedel, D.; Roszak, A. W.; McKendrick, K.; McAuley, K. E.; Fyfe, P. K.; Nabedryk, E.; Breton, J.; Robert, B.; Cogdell, R. J.; Isaacs, N. W.; Jones, M. R. *Biochim. Biophys. Acta* **2002**, *1554*, 75−93.

(23) Czarnecki, K.; Cua, A.; Kirmaier, C.; Holten, D.; Bocian, D. F. *Biospectroscopy* **1999**, *5*, 346−357.

(24) (a) Youvan, D. C.; Ismail, S.; Bylina, E. J. *Gene* **1985**, *33*, 19−30. (b) Bylina, E. J.; Ismail, S.; Youvan, D. C. *Plasmid* **1986**, *16*, 175−181. (c) Bylina, E. J.; Jovine, R. V. M.; Youvan, D. C. *Bio/Technolgy* **1989**, *7*, 69−74. (d) Kolaczkowski, S. V.; Bylina, E. J.; Youvan, D. C.; Norris, J. R. In *Molecular Biology of Membrane-Bound Complexes in Photosynthetic Bacteria*; Drews, G., Ed.; Plenum: New York, 1990; pp 305−312.

(25) (a) Kirmaier, C.; Holten, D. *Biochemistry* **1991**, *30*, 609−613. (b) Yang, S. I.; Li, J.; Cho, H. S.; Kim, D.; Bocian, D. F.; Holten, D.; Lindsey, J. S. *J. Mater. Chem.* **2000**, *10*, 283−296.

(26) (a) Shreve, A. P.; Cherepy, N. J.; Mathies, R. A. *Appl. Spectrosc.* **1992**, *46*, 707−711. (b) Cherepy, N. J.; Shreve, A. P.; Moore, L. J.; Franzen, S.; Boxer, S. G.; Mathies, R. A. *J. Phys. Chem.* **1994**, *98*, 6023−6029.

(27) (a) Cherepy, N. J.; Holzwarth, A.; Mathies, R. A. *Biochemistry* **1995**, *34*, 5288−5293. (b) Cherepy, N. J.; Shreve, A. P.; Moore, L. J.; Boxer, S. G.; Mathies, R. A. *J. Phys. Chem. B* **1997**, *101*, 3250−3260.

(28) (a) Palaniappan, V.; Schenck, C. C.; Bocian, D. F. *J. Phys. Chem.* **1995**, *99*, 17049−17058. (b) Czarnecki, K.; Diers, J. R.; Chynwat, V.; Erickson, J. P.; Frank, H. A.; Bocian, D. F. *J. Am. Chem. Soc.* **1997**, *119*, 415−426. (c) Czarnecki, K.; Chynwat, V.; Erickson, J. P.; Frank, H. A.; Bocian, D. F. *J. Am. Chem. Soc.* **1997**, *119*, 2594−2595.

(29) (a) Wachtveitl, J.; Farchaus, J. W.; Das, R.; Lutz, M.; Robert, B.; Mattioli, T. A. *Biochemistry* **1993**, *32*, 12875−12886. (b) Mattioli, T. A.; Williams, J. C.; Allen, J. P.; Robert, B. *Biochemistry* **1994**, *33* 1636−1643. (c) Mattioli, T. A.; Lin, X.; Allen, J. P.; Robert, B. *Biochemistry* **1995**, *34*, 6142−6152.

(30) (a) Breton, J. *Biochim. Biophys. Acta* **1985**, *819*, 235−245. (b) Breton, J.; Bylina, E. J.; Youvan, D. C. *Biochemistry* **1989**, *28*, 6423−6429.

(31) (a) Palanniappan, V.; Bocian, D. F. *J. Am. Chem. Soc.* **1995**, *117*, 3647−3648. (b) Czarnecki, K.; Schenck, C. C.; Bocian, D. F. *Biochemistry* **1997**, *36*, 14697−14704.

(32) Goldsmith, J. O.; King, B.; Boxer, S. G. *Biochemistry* **1996**, *35*, 2421−2428.